Journal of Materials and
Environmental Sciences
ISSN : 2028-2508

JMES, 2017 Volume 8, Issue 10, Page 3598-3607

http://www.jmaterenvironsci.com /

Electrochemical performance of the V_2O_5 and VO_2 thin films synthesized by spray pyrolysis technique

A. Mrigal[1]*, M. Addou[1], M. El Jouad[2] and S. Khannyra[1]

[1] *Laboratory Optoelectronics and Physical Chemistry of Materials. Ibn Tofail University, Faculty of Science BP 133 14000 Kenitra, Morocco.*

[2]*The Engineering Sciences Laboratory for Energy, National Engineering School of Applied Science. Chouaib Doukkali University of El Jadida, BP : 1166 El Jadida Plateau 2400, Morocco.*

Received 28 Feb 2017,
Revised 15 Apr 2017,
Accepted 20 Apr 2017

Keywords
✓ Vanadium pentoxide V_2O_5;
✓ Electrochemical;
✓ Vanadium dioxide (VO_2); VO_2(M); VO_2(B);
✓ Spray pyrolysis.

mrigalasmaa@gmail.com,

Abstract

In this study, we focus on the thin films growth based on vanadium oxide using the chemical reactive liquid spray technology (RCSLP) deposited on glass substrates. The flow rate was set at 1.5 ml/min, the substrate temperature at 450°C, the deposition time at 10 min and then the solution concentration at different values (0.05M, 0.025M and 0.015M). The influence of all these parameters on the structural and optical properties of thin films of V_2O_5 and VO_2 was carefully studied. The decrease of the solution molar concentration from C=0.05M to C=0.015M was conducted to transform V_2O_5 to VO_2(B) and then VO_2(M). The transparency has increased from 14% to 70% while changing the concentration of solution from 0.05M to 0.015M. The electrochemical behavior was investigated in (0.5 M $LiClO_4$ propylene carbonate (PC)) solution using a three-electrode cell. The results of the XRD diagrams, the SEM images, the electrical measurement and the spectral transmission show clearly the transformation of V_2O_5 to VO_2(B) and then VO_2(M).

1. Introduction

The materials for positive electrodes must have high electronic and ionic conductivity, good chemical stability towards the electrolyte, high standard potential versus Li/Li^+ pair, reversibility of the intercalation reaction which requires the stability of the host network, and a large ratio of number of cationic sites available per the molecular weight allowing a wide range of intercalation.

In the field of cathode materials, the first research has been directed towards compounds having a lamellar structure such as the transition elements of Groups IV, V, VI, X.

The vanadium oxides and their composites have been extensively studied due to their structure, chemical and physical properties, which lead them to have a wide range of practical applications. As an example of vanadium oxides, we find vanadium pentoxide V_2O_5, and vanadium dioxide (VO_2) [1-9].

The thin layers of vanadium pentoxide V_2O_5 have been the subject of research in recent years due to their wide variety of applications involving optical switching [10] and electrochemical devices. Indeed, high electrochemical activity, high stability and ease of vanadium oxide thin films formation by numerous deposition techniques led to its use as lithium batteries with high capacity [11] and as transparent anode in solar cells. Vanadium pentoxide is characterized by a layered structure in which small alkaline atoms may be reversibly intercalated and deintercalated. In the particular case of lithium, up to three ions per V_2O_5 unit may be inserted and extracted, so providing an overall capacity of about 440 $mAh.g^{-1}$ in the potential range 3.8–1.5 V [2-3].

The vanadium dioxide (VO_2) is a binary composite. It has different polymorphs, including VO_2(M), VO_2(R), VO_2(B), VO_2(A), VO_2(C) [14]. In addition to VO_2, the vanadium-oxygen phase diagram shows nearly 20 other stable phases of vanadium oxide. Coupled with these diverse forms of vanadium oxide, the formation of VO_2 occurs only in a very narrow range of oxygen partial pressure [13-14]. Many VO_2 phases have been reported, including VO_2(A), VO_2(B), VO_2(R), and VO_2(M) [15]. Among them, VO_2(M) is the most important because it shows a first order transition metal insulator fully reversible with the phase transition temperature

(Tc) at approximately 68°C, followed also by a crystallographic transition, accompanied by a crystallographic transition between a low temperature monoclinic phase (M) and a high temperature rutile phase (R) [16-17].

In this article, we present V_2O_5 and VO_2 films prepared by Reactive Chemical Spraying technology in Liquid Phase (RCSLP). The structure, morphology and the desirable optical electrical and electrochemical property were obtained with high yields by adjusting several key parameters to control the chemistry of materials. To obtain a stable phase of VO_2(M) and V_2O_5, several parameters were varied.

2. Materials and methods

We growth our thin films based on V_2O_5 and VO_2, from an aqueous solution containing vanadium chloride (VCl_3) using the spray pyrolysis method. They are deposited onto glass substrates heated at 450°C, the solution concentration were 0.05M, 0.025M and 0.015M, the deposition time was 10min, and the flow rate was fixed at 1.5ml/min. The experimental set-up for this last has been described previously [18].

The structural characterizations are performed using X-ray diffraction (XRD) with Cu Kα radiation (λ=1.5406 Å), the patterns were recorded over the angular range 13–80° (2θ). Morphology of deposited thin films was observed using FEI Quanta 200 Brand scanning electron microscope. Optical measurements were carried out using the Spectrophotometer JASCO UV/VIS/NIR V570 in the wavelength range (350 - 2200nm). Electrical measurements were carried out using the Multimeter JEULIN CL 3015. The electrochemical experiments were performed using a VoltaLab system withVM4. A platinum sheet was used as a counter electrode. The potential was measured with respect to the saturated calomel reference electrode (SCE).

3. Results and discussion

Figure 1 shows the XRD patterns for samples grown at deposition time 10 min for different solution molar concentration C=0.05M, C=0.025M, C=0.015M and deposited at Ts=450°C.

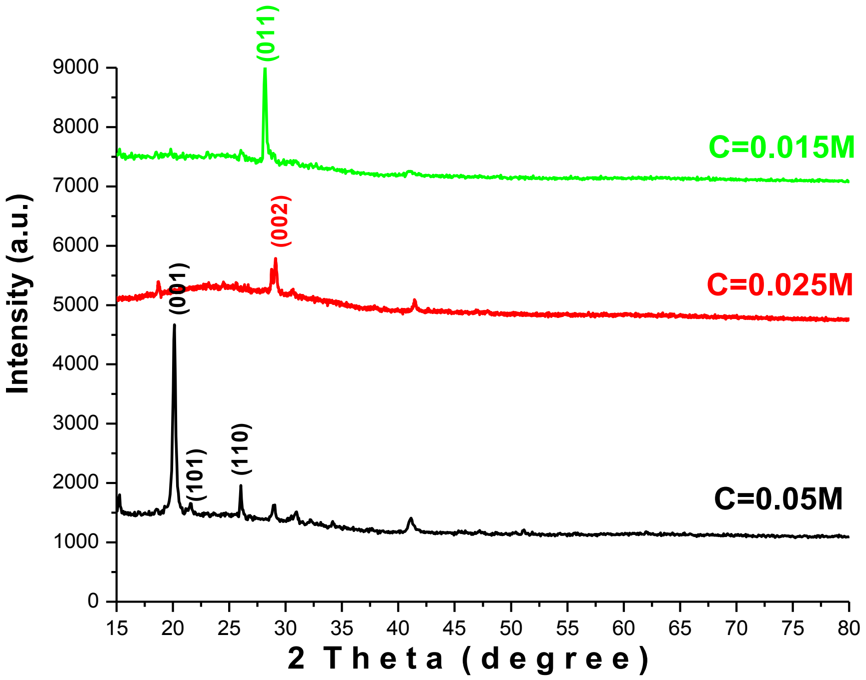

Figure 1: X-ray diffraction spectra of V_2O_5 and VO_2 samples at different solution concentration.

Analysis by X-ray diffraction showed that all layers are polycrystalline. The films prepared at C = 0.05M have orthorhombic structure and the preferred orientation of thin V_2O_5 (001) at the angle 2θ=20.07°, indicates the preferred orientation along the crystallographic C axis perpendicular to the substrate and which is the main line of the orthorhombic structure the lattice parameters a=11.382Å, b=3.575Å, c=4.422Å. The complete conversion from V_2O_5 to VO_2(B) was observed when we changed the molar solution concentration from 0.05M to 0.025M. The sample prepared at C = 0.025M is crystallized according to the plan (002) at an angle 2θ =29°. Films prepared at C = 0.015M show a peak (011) more intense at an angle 2θ =27.96° [12] and have monoclinic structure. The cell parameters of the room temperature phase VO_2(M) are a=5.744Å, b=4.517Å, c=5.38 Å, β=102.6°, Z=4, the space group is P21/c (JCPDS card No.72-0514). These results show that the transformation of VO_2 phase (B) to VO_2 (M) was made successfully.

The effect of the concentration (C=0.05M, C=0.025M, C=0.015M) on the morphology of the material is clearly visible in Figure 2. The Figure 2a shows the evolution of morphology of V_2O_5 thin films with 0.05M concentration, the deposited V_2O_5 film has a very porous nature, and particle shape is three-dimensional. Figure 2b shows the morphology of VO_2 films with C=0.025M, we observe nanorods of vanadium dioxide VO_2(B). Figure 2c shows images of VO_2 (M) obtained at C=0.015 M. The vanadium dioxide materials have a similar shape with a larger rod [19].

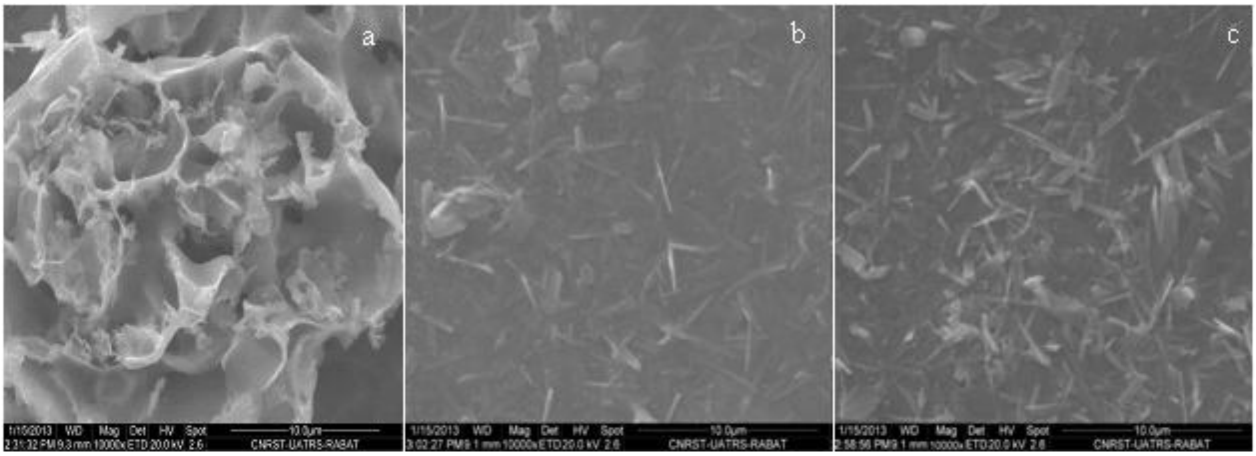

Figure 2: SEM of V_2O_5 and VO_2 samples at different solution concentration of (a) 0.05M (V_2O_5), (b) 0.025M (VO_2) and (c) 0.015M (VO_2).

We present in Figure 3 spectral transmission for V_2O_5 and VO_2 with different solution molar concentration C=0.05M, C =0.025M and C=0.015M. All films were deposited at 450°C heated substrates and deposition time of 10 min. The Optical transmission of thin films was measured in the range 300 – 2000nm using a spectrophotometer at room temperature.

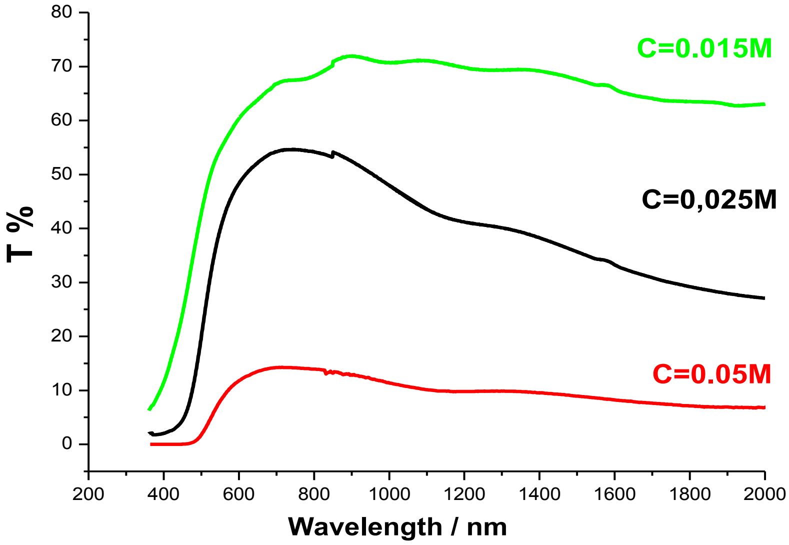

Figure 3: Transmission spectra of V_2O_5 and VO_2 samples at concentration of the solution 0.05M (V_2O_5), 0.025M (VO_2) and 0.015M (VO_2).

For the concentration of C=0.05M the spectra shows a gap of 14% in the visible region and a slight decrease in the near-infrared range (NIR), the transmission was low because of the high concentration. The same results were reported by Bouzidi et al. [21]. The spectral transmission of VO_2 films prepared with these conditions C=0.025M, shows a gap of 54%, in the visible region and a slight decrease in the near-infrared range (NIR), the transmission increases with the decrease of the concentration.

The concentration increase of free electrons in the thin films conducts to a decrease of NIR region. The transmittance in the infrared zones is also inversely related to the concentration due to the interaction between free electrons and the incident long wavelength [22].

For the C=0.015M the spectra shows a gap of 67% in the visible region and a slight increase in the near-infrared range (NIR) 72%.The same results were reported by Yuankai Liu et al. [23].
The optical absorption coefficient (α) is calculated from the relation:

$$\boldsymbol{\alpha = \frac{1}{t\left[ln(\frac{100}{T})\right]}}$$

Where, T is the measured transmittance and t is the film thickness. By linear fitting and extrapolating the line to the abscissa (Plot of $(\alpha h\nu)^2$ vs $(h\nu)$), we can get the direct band gap (Eg) (Figure 4).The solution concentration (C=0.05M, C=0.025M, C=0.015M) influences clearly the direct gap energy. We noticed that the direct optical gap decreased when increasing the solution molar concentration, at C= 0.015 M for Eg = 2.66ev, C = 0.025M for Eg = 2.46ev and C = 0.05M for Eg = 2.44ev.

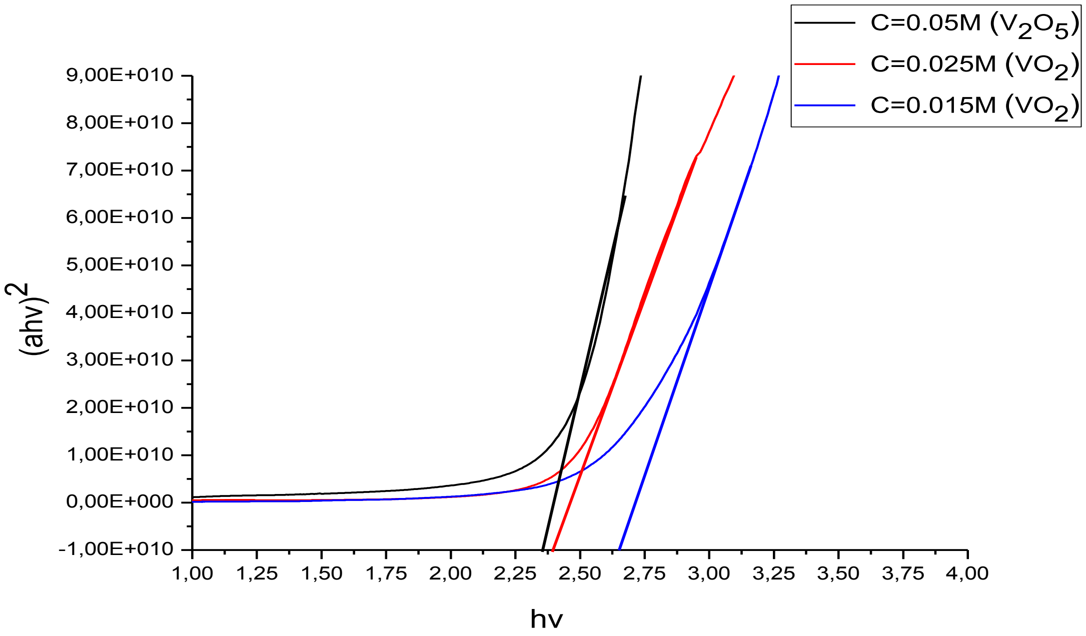

Figure 4: Direct band gap estimation at concentration of the solution 0.05M (V_2O_5), 0.025M (VO_2) and 0.015M (VO_2).

The effect of the molar concentration of the solution (C = 0.05M, C = 0.025 M, C = 0.015 M) over the electric properties at ambient temperature presented in Figure 5. The resistivity decreases with increasing concentration of the solution [24].

The electrochemical measurements are carried out using the three-electrode cell. This cell is used for measuring the current injected or extracted from the layers during intercalation / extraction of Li^+ ions in various potential (cyclic voltammetry).

The applied potential between the electrode and reference one varies between -1 V/ SCE and +2V/ SCE. The application cathode potential (-1V/SCE) causes insertion of electrons and lithium ions in the layer while the anode potential application (2V/ SCE) results in their extraction.

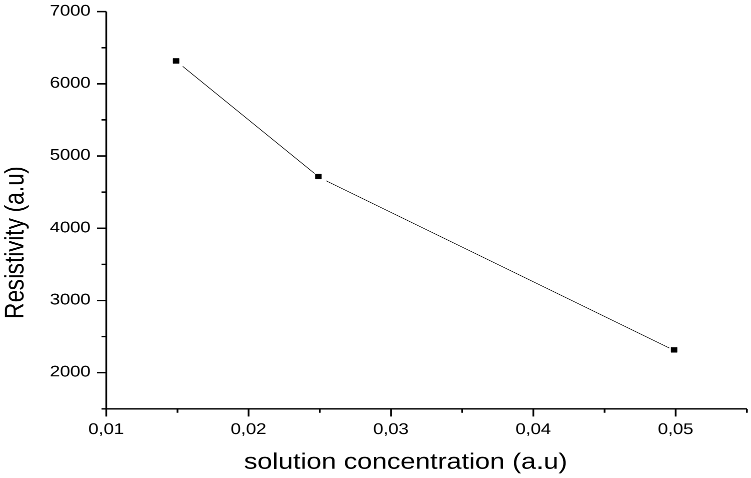

Figure 5: Resistivity at concentration of the solution 0.05M (V_2O_5), 0.025M (VO_2) and 0.015M (VO_2).

Figure 6 shows the first cycle of voltammogram between -1V/SCE and +2V/SCE [25] of V_2O_5/ITO and VO_2/ITO thin film elaborated at substrate temperature of 450 °C with different concentration of the solution at scan rate V = 50 mV/s.

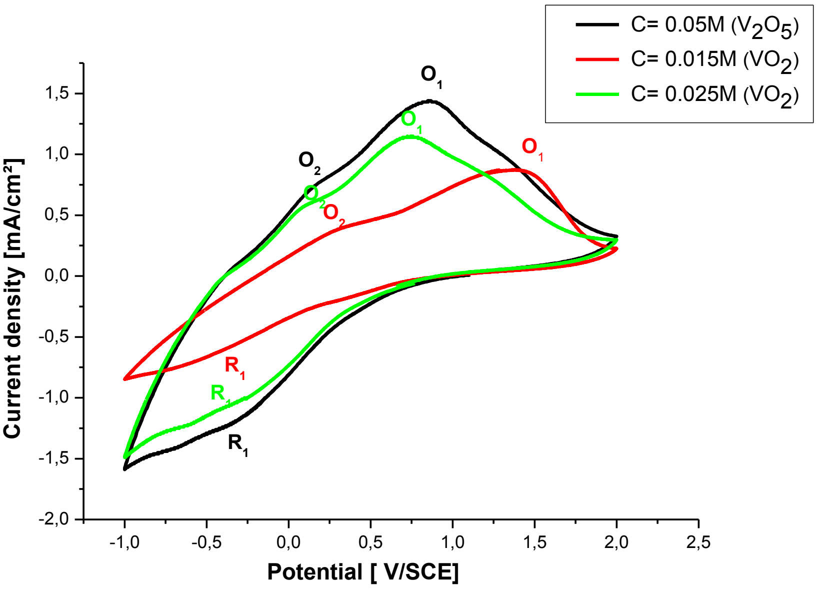

Figure 6: Cyclic voltammogram of V_2O_5 and VO_2 on ITO glass, electrode in the potential range of -1 to +2V/SCE

The observed peaks characterize the electrochemical reactions which follow the insertion of lithium ions within the material. The tops of these peaks are represented by these arrows in Figure 6. The current intensity measured at the top of each peak is denoted Ip and is usually called "current peak".

$$Ip=2.69*10^5 n^{3/2} D_{Li}^{1/2} C_{Li}*v^{1/2}$$

Where Ip represents the peak current density (A/cm^2), n is the number of electrons per reaction species (1 for Li^+), D_{Li} is the solid state diffusion coefficient of Li^+, C_{Li} is the maximum concentration of Li^+ within the electrode and v is the speed of potential sweep.

In the typical case of the films of V_2O_5 and VO_2, the voltammogram is shown in Figure 6, there are two oxidation peaks (O_1, O_2) and a reduction peak R_1 [26].

Negative currents correspond to a phenomenon of reduction of the transition metal followed by the insertion of Li^+ while positive currents are the evidence of oxidation of the transition metal and thus the extraction of lithium ion.

The process of intercalation/extraction is realized electrochemically according the following cathodic/anodic reaction:

$$V_2O_5 + x\,Li^+ + x\,e^- \Leftrightarrow Li_xV_2O_5$$
$$VO_2 + x\,Li^+ + x\,e^- \Leftrightarrow Li_xVO_2$$

The cycle opening of V_2O_5 films indicates that the layer promotes the process of intercalation/ extraction of Li^+ ions, in agreement to several studies.

Several sweep cycles are carried out with the same perturbation of the electrode. This process makes it possible to determine the rank of the cycle from which we can observe a good reproducibility of experimental curves. This reproducibility is explained by the stability of the activity of the substrate surface. In our case, this study allows us to have a deep understanding regarding the stability of the thin film of vanadium oxide in the supporting electrolyte ($LiClO_4$).

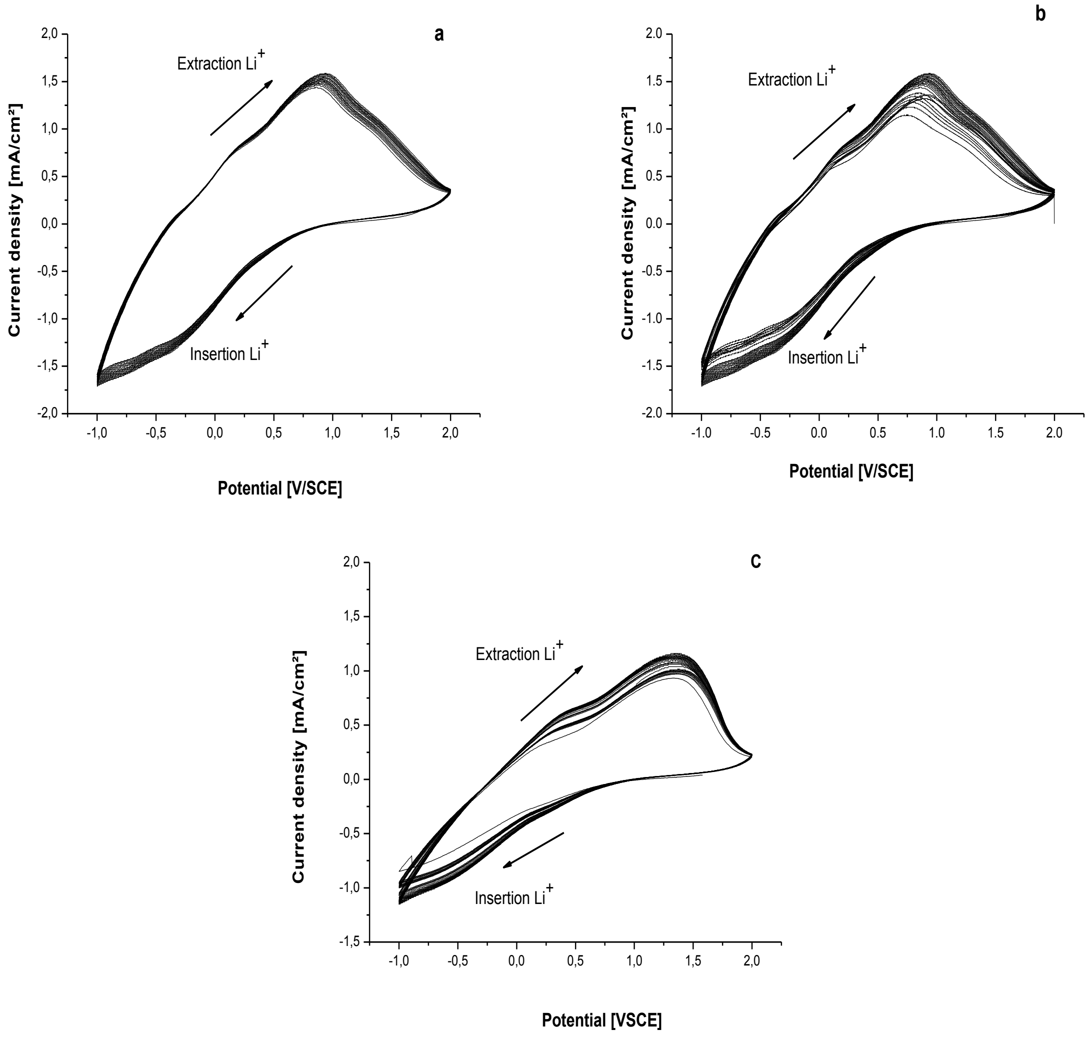

Figure 7: cyclic voltammograms of a thin layer of V_2O_5 and VO_2 during 50 cycles (0.5M ($LiClO_4$), V=50mV/s) (a) 0.05M (V_2O_5), (b) 0.025M (VO_2) and (c) 0.015M (VO_2).

The Figure 7 represents cyclic voltammograms films of V_2O_5 and VO_2 recorded during 50 cycles. We notice that the cycles of the V_2O_5 layer are repeatable and no reduction in the current density was recorded.

The Figure 8 shows the evolution of the capacity during 200 cycles for the thin layers of V_2O_5 and VO_2. The thin films of V_2O_5 have a higher capacity than VO_2.

They have a good cycling performance; the capacity is passing from 257 $mAh.g^{-1}$ at the 1st cycle to 246 $mAh.g^{-1}$ at the 200th cycle, and a low capacity loss of 4.28% at the 200th cycle. The amount of charge injected when we apply the cathodic potential of -1.5 V/SCE for 1 min is 1.75 mC and the calculated intercalation rate x is about 2.3 Li/ V_2O_5.

The thin layers of VO_2 prepared at C = 0.025M show a loss of capacity of about 12.7% at the 200th cycle (capacity is passing from 197 $mAh.g^{-1}$ to 172 $mAh.g^{-1}$) while those prepared at C = 0.015M present a capacity loss of 4.54% at the 200th cycle (capacity value is 132$mAh.g^{-1}$ at the 200th cycle).

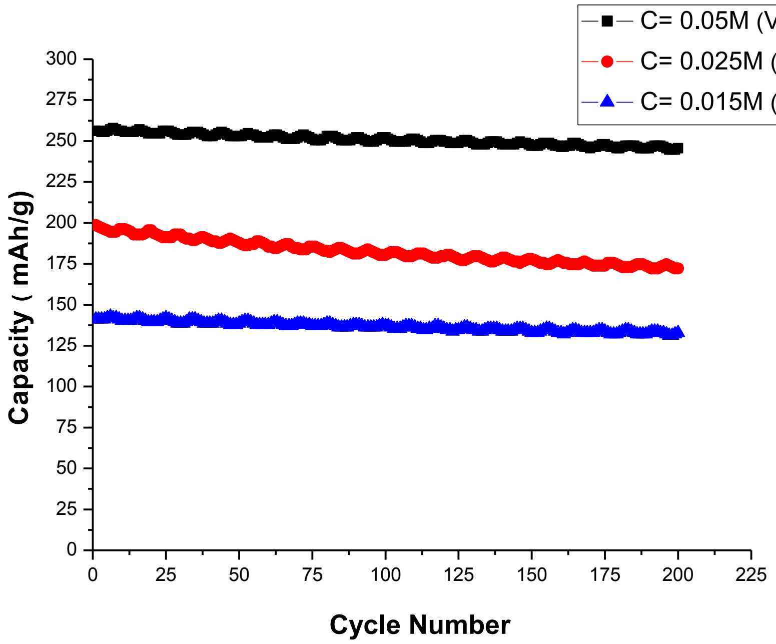

Figure 8: Capacity versus cycle number for the V_2O_5 and VO_2 electrodes between -1 and 2 V/SCE.

Conclusions

The vanadium oxide V_2O_5, VO_2(B) and VO_2(M) were prepared successfully using the technology of chemical reactive liquid spray (RCSLP). The substrate temperature 450°C, the deposition time 10 min and the concentration of the solution (0.005M, 0.025M and 0.015M) have been identified as the most important parameters to control the result of crystalline phase and its morphology. The interaction between the different polymorphs of VO_2 is extremely sensitive to the conditions of the elaboration. The results of the XRD diagrams, SEM images, electrical properties, and spectral transmission show clearly that the films of VO_2 (M) have been successfully elaborated at Ts=450°C, C=0.015M and t= 10min.The electrochemical properties show that V_2O_5 thin films lead to a high capacity of insertion / extraction of lithium ions.

Acknowledgments-This work is supported by Hassan II Academy of Science and Technology, Action MA/228 and the CNRST-URAC-14, PPR/2015/9- Morocco.

References

1. Zhang Y., Fan M., Liu X., Xie G., Li H., Huang C., *Solid State Commun.* 152 (2012) 253.
2. Tranchant A., Messina R., Perrichon J., *J. Electroanal. Chem.* 113 (1980) 225.
3. Ragupathy P., Shivakumara S., Vasan H.N., Munichandraiah N., *J. Phys. Chem. C* 112 (2008) 16700.
4. Mrigal A., Addou M., Khannyra S., El Jouad M., *Int. J. Adv. Res. Phys. Sci.* 8 (2015) 24–29.
5. Zhang Y., Li W., Fan M., Zhang F., Zhang J., Liu X., Zhang H., Huang C., Li H., *J. Alloy. Compd.* 544 (2012) 30.
6. Whittaker L., Jaye C., Fu Z.G., Fischer D.A., Banerjee S., *J. Am. Chem. Soc.* 131 (2009) 8884.
7. Qian K., Shaotang L., Shidong J., Wenjing L., Yamei L., Chen R., Jin P., *Ceram. Int.* 40 (2014) 14517–14521.
8. Navone C., Pereira-Ramos J.P., Baddour-Hadjean R., Salot R., *J. Power Sources* 146 (2005) 327–330

9. Zhang Y., Zhang X., Huang Y., Huang C., Niu F., Meng C., Tan X., *Solid State Commun.* 180 (2014) 24–27.
10. Livage J., Guzman G., Beteille F., Davidson P., *J. Sol-Gel Sci. Techn.* 8 (1997) 857–865.
11. Zhaang J.G., Mc Graw J.M., Turner J., Ginley D., *J. Electrochem. Soc.* 144 (1997) 1630–1634.
12. Hagrman D., Zubieta J., Warren C. J., Meyer L.M., Treacy M.M.J., Haushalter R.C., *J. Solid State Chem.* 138 (1998) 178.
13. Nag J., Haglund Jr R. F., *J. Phys-Condens. Mat.* 20 (2008), 264016.
14. Balu R., Ashrit P. V., *Appl. Phys. Lett.* (2008), 92, 021904.
15. Alie D., Gedvilas L., Wang Z., Tenent R., Engtrakul C., Yan Y., Shaheen S. E., Dillon A. C., Ban C., *Solid State Chem.* S0022-4596 (2013) 00480–5.
16. Zhang Y., Fan M., Niu F., Wu W., Huang C., Liu X., Li H., Liu X., *Curr. Appl. Phys.* 12 (2012) 875 .
17. Zhang Y., Zhang J., Zhang X., Huang C., Zhong Y., Deng Y., *Mater. Lett.* 92 (2013) 61.
18. Addou M., Moumin A., Elidrissi B., Regragui M., Bougrine A., Kachouane A., Monty C., *J. Chem. Phys.* 96 (1999) 232.
19. Yifu Z., Juecheng Z., Xiongzhi Z., Yuan D., Yalan Z., Huang C., Xin L., Xinghai L., Shaobo M., *Ceram. Int.* 39 (2013) 8363–8376.
20. Lili Z., Lei M., Sakae T., Jianhua Z., Lihua C., Xiudi X., Gang X., *Thin Solid Films* 543 (2013) 157–161.
21. Bouzidi A., Benramdane N., Nakrela A., Mathieu C., Khelifa B., Desfeux R., Da Costa A., *Mater. Sci. Eng., B,* 95 (2002) 141–147.
22. Fellahi N., Addou M., Sofiani Z., El jouad M., Bahedi K., Bayoud S., Haouti M., sahraoui B., bernede J.C., *J. optoelectron. adv. m.,* (2010), 1087–1091.
23. Yuankai L., Haizheng T., Xinhong C., Meinan W., Jianhua B., Xiujian Z., *J. Non-Cryst. Solids* 383 (2014) 116–120.
24. Alaa A., Akl, *Appl. Surf. Sci.* 252 (2006) 8745–8750.
25. Yanning L., Chun yang J., Zhongquan W. ,Xiao long W., Jianliang X., Longjiang D., *Sol. Energ. Mat. Sol. C.* 132 (2015) 467–475.
26. Zhongqiu T., Na L., Haiming L., Yanlong T., Qu H., Zhang X., Zhao J., Yao L., *Sol. Energ. Mat. Sol. C.* 146 (2016) 135–143.

(2017) ; http://www.jmaterenvironsci.com/